

The Main Injector Particle Production Experiment

Holger Meyer

Wichita State University, Wichita, KS 67260, USA

Abstract

It is currently impossible to apply the theory of strong interactions, QCD, to compute non-perturbative hadron interaction cross sections from first principles. Thus high quality hadronic particle production measurements are needed to fully understand the data from experiments that have hadronic interactions as a signal or background. This includes atmospheric and accelerator neutrino experiments, calorimetry and hadronic shower simulation. Such data can also be used to test observed regularities in particle production such as scaling relations in inclusive reactions with some precision. The spectrum of baryon resonances predicted by QCD includes many states that have not been observed. Measurements of pion, kaon, and proton beams on a liquid hydrogen target at beam momenta around 1 GeV/c will provide important input to searches for missing baryon resonances.

We review status, results, and prospects of particle production measurements at Fermilab.

Key words: MIPP, hadron production, experiment

1. Introduction

The physics goals of the Main Injector Particle Production (MIPP) experiment have been described in [1]. The need for hadron production measurements with good particle identification has been summarized in [2], at this conference, and elsewhere. The proceedings of the Hadronic Shower Simulation Workshop HSSW06 [3] contain comparisons of common hadronic shower simulation packages that show large discrepancies between different models in regions of phase space where data is sparse or unavailable. Here we briefly summarize the motivation for the MIPP experiment and focus in more detail on the data reconstruction, quality and quantity of MIPP data, and planned upgrades to the experiment.

Hadron production data has many uses. These include improvements in knowledge of the spectrum of accelerator neutrino beams produced by decaying pions and kaons, hadronic shower simulation for calorimetry applications, and data needed to aid in the design of future experiments. The success of an international linear collider depends (among other things) on excellent calorimeter resolution ($30\%/\sqrt{E}$) of the ILC detector to distinguish WW and ZZ events. Currently we cannot apply QCD to compute cross sections. QCD events are either signal or background to practically every particle physics experiment. Thus the current understanding

of QCD cross sections is deeply dissatisfying. In order to advance the field new high statistics, low systematics data are needed to allow theorists to test new theories and to identify patterns in the cross sections. One such pattern, a general scaling law of particle fragmentation [4], will be tested using MIPP data.

The MIPP beam momentum range extends down to 5 GeV/c in the current data set, but can be extended down to 1 GeV/c [6]. This puts searches for unobserved baryon resonances in the reach of a future MIPP run. The use of six types of beams, baryons and mesons, strange and non-strange, in the same detector may enhance signals that could be missed by other experiments.

Part of the MIPP data run was dedicated to a novel technique to measure the charged kaon mass [10]. The charged kaon mass measurement world average [5] is dominated by two measurements that significantly deviate from one another. A new measurement is needed to resolve this disagreement. A measurement with a new technique is especially useful as it avoids any common systematics with either of the other two measurements. In the MIPP experiment charged kaons of known momentum can be produced in the beam line. The momentum can be measured precisely in the MIPP spectrometer and the velocity of the same kaon is measured by the radius of the RICH ring with high precision. The kaon

mass is derived from these two measurements.

The MIPP experiment also addresses topics in nuclear physics (nuclear γ -scaling, propagation of flavor through nuclei, etc.). These have been described before [1].

2. MIPP experiment overview

The Main Injector Particle Production experiment measures charged particle production cross sections of beams of pions, kaons, and protons of both charges on fixed nuclear targets ranging from liquid hydrogen to uranium and the composite NuMI target used by the MINOS experiment at Fermilab. The beams are generated in the Fermilab Meson Center area using $120\text{GeV}/c$ protons from the Main Injector. Particles produced in the reactions are tracked and identified in the detector consisting of a TPC and tracking chambers, multicell threshold Čerenkov detector, time of flight wall, RICH, and calorimeter. The beam momentum can be adjusted from $5\text{GeV}/c$ to $90\text{GeV}/c$. The experiment recorded 18 million events of cross section data in a 14 months physics run in 2005/2006. Approximately 14 million events for the kaon mass measurement were also recorded.

3. The MIPP spectrometer and beamline

Figure 1 shows the MIPP beam line [7]. Using slow extracted $120\text{GeV}/c$ protons from the Main Injector the beam line produces a stream of tagged π^+ , K^+ , and protons or π^- , K^- , and anti-protons at the selected momentum. These secondary beams travel 96 meters between the primary and experimental targets and get identified in a set of two differential beam Čerenkov detectors (BCKov). The gas pressure in the BCKovs is adjusted as shown in figure 2. BCKovs and Beam time of flight give excellent beam particle identification for all beam momenta. The beam particle identification purity is directly measured with the MIPP detector for beam particles that do not interact in the 1% interaction length experimental targets. It is typically $> 80\%$ for the minority particle and close to 100% for the majority particles. The trigger prescales beam species to record the same number of event for all three types of beam particles. The experiment can also receive $120\text{GeV}/c$ proton beam. The primary target is removed in this setup.

The MIPP detector is shown in figure 3. Particles are tracked through the TPC and six wire chambers with four planes each in the magnetic fields of the JGG and Rosie magnets and identified in the TPC ($\sim 0.1\text{GeV}/c$

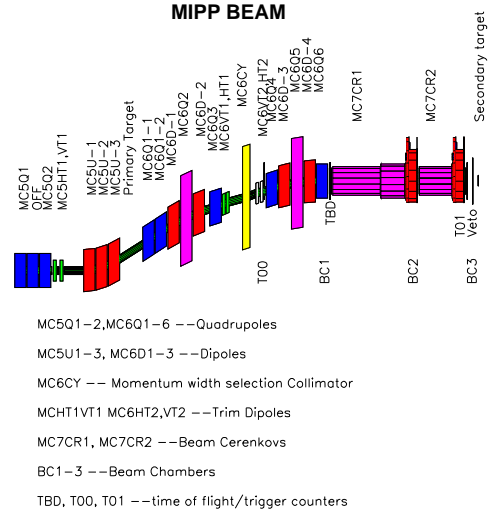


Figure 1: Side view of the MIPP beam line.

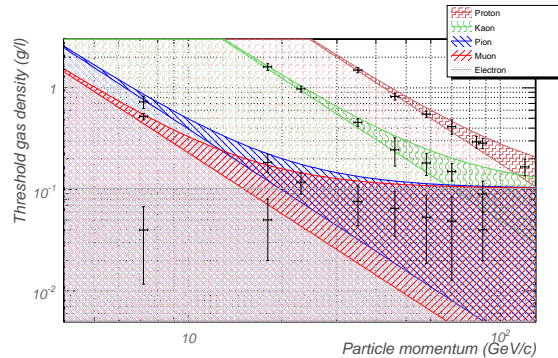


Figure 2: Beam Čerenkov density curves.

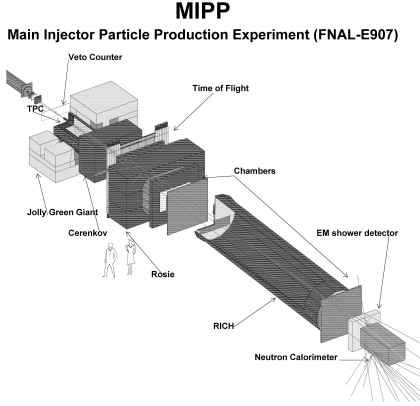


Figure 3: The MIPP detector.

to $\sim 1\text{GeV}/c$), ToF ($\sim 1\text{GeV}/c$ to $\sim 2.5\text{GeV}/c$), Ckov ($\sim 2.5\text{GeV}/c$ to $\sim 17\text{GeV}/c$), and RICH ($\sim 17\text{GeV}/c$ to $\sim 100\text{GeV}/c$). A calorimeter [11] for particles with low transverse momentum completes the detector. Interactions are triggered using a small scintillator just downstream of the target, supplemented by multiplicity in the first drift chamber.

4. Data reconstruction

To reconstruct events data from the TPC and tracking chambers is first used to form track segments. Tracks get formed using a template method. Then vertices are formed using a deterministic annealing filter. In a final step all tracks and vertices are re-fit using vertex constrained fits. In order for these steps to succeed, the detectors have to be aligned by minimizing track residuals, the magnetic fields of both analysis magnets have to be known precisely, and $E \times B$ distortions arising from magnetic field components perpendicular to the 10kV electric field in the TPC have to be corrected. To this end the electron drift in the P10 gas mixture in the TPC drift volume has been modeled using the MagBoltz code and parametrized as a function of electron drift velocity v_0 , angle between \vec{B} and \vec{E} , and strength of the magnetic field. The drift velocity is calibrated run by run and correlates strongly with the water vapor contamination in the P10 gas. The magnetic field of the Jolly Green Giant magnet is not very uniform (figures 4,5) and the corrections are large. A linear drift model previously used by other experiments did not reproduce the MIPP data. This careful work has been rewarded with a track momentum resolution of $dp/p \leq 5\%$ and vertex

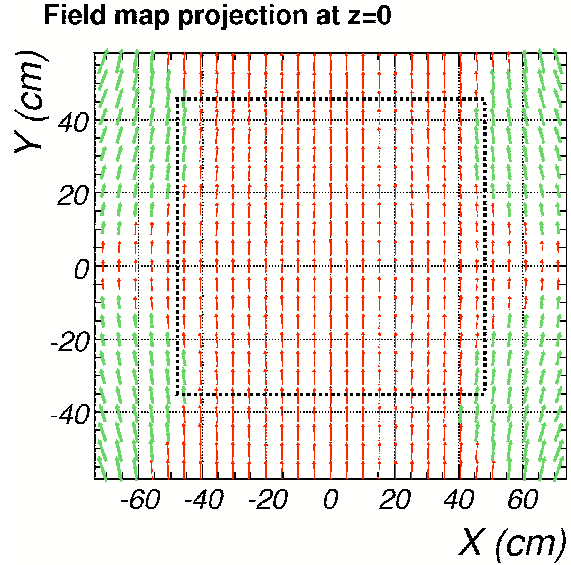


Figure 4: The Jolly Green Giant magnetic field plotted at the center of the magnet in z .

position resolution of $\sim 6\text{mm}$ along the beam direction (the z axis) and $\sim 1\text{mm}$ along the x and y directions.

Once all tracks have been found the identity of the particles is established from dE/dx in the TPC, time of flight to the ToF wall, and Čerenkov response in Ckov and RICH detectors. Each of these detectors provides a log-likelihood for each particle hypothesis. In a final step the individual sub-detector log-likelihoods are combined into a global log-likelihood PID. This is an iterative process because the prior particle fractions are approximations and particle fractions depend on the data sample. This rigorous approach to particle identification is necessary especially for the minority particles and in regions of overlap between different sub-detectors. Preliminary results have been obtained with simple cut-based analyses.

The calibration of the particle identification detectors was involved. The ToF wall calibration was complicated by the fact that the cable delay changed with environment temperature and had to be calibrated using $\beta = 1$ particles. This was hard to do for parts of the ToF wall with low occupancy. The RICH detector was studied most carefully. Rings typically have a large number of hits and can ring center and radius can be fit with high precision (figure 6).

The MIPP data and detector provide many opportunities for internal consistency checks. In p-p interactions the results must be invariant under exchange of the beam proton with the fixed target proton. Thus the

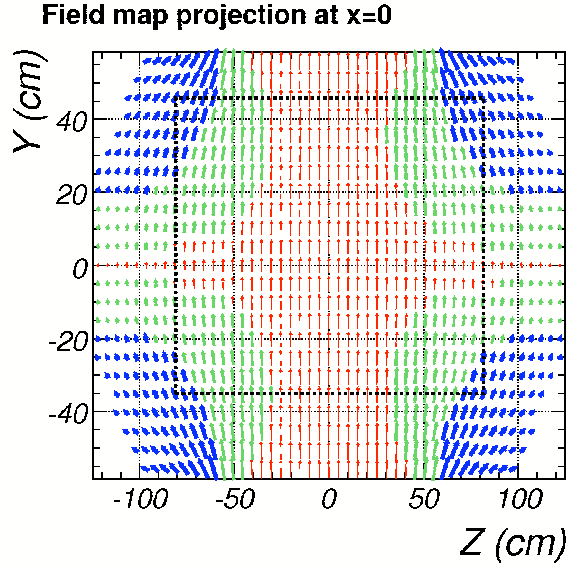


Figure 5: The Jolly Green Giant magnetic field plotted at the center of the magnet in x . The experimental target is just to the left of $y=0$ in this plot. Distortions between this region and the pad plane at the bottom influence vertex reconstruction most.

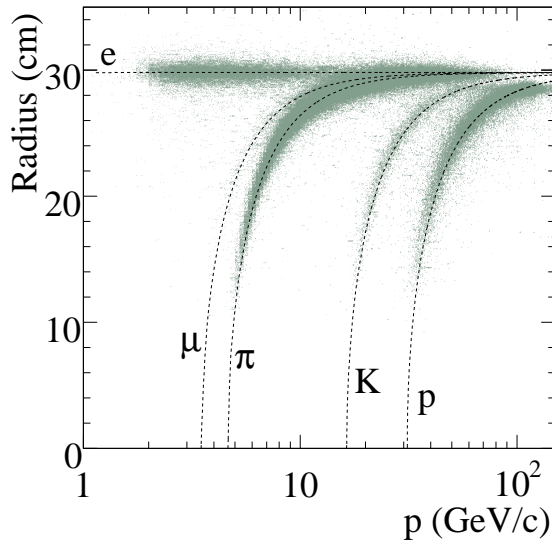


Figure 6: RICH ring radius vs. particle momentum. The lines are predictions for each particle type.

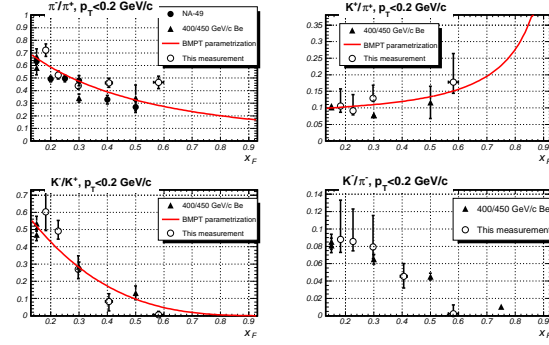


Figure 7: Ratios of π s and K s produced in reactions of $120\text{GeV}/c$ protons on a carbon target for $p_T < 0.2\text{GeV}/c$.

low energy, large angle particles originating from reactions of the target proton can be compared to high energy, small angle particles originating from the beam proton and the acceptance and momentum resolution of large angle tracks in the TPC can be checked against forward-going tracks that get identified in the Ckov and RICH detectors. The beam PID purity can be checked directly with the downstream detectors for uninteracted beam particles. The quality of the existing MIPP data is good. The physics output is limited by the available man-power.

5. Results

Three PhD theses [8, 9, 10] have been completed and several preliminary results, including preliminary cross sections, have been shown. Figures 7 to 10 from [8] show ratios of π s and K s produced in reactions of $120\text{GeV}/c$ protons on a carbon target in different bins of p_T and compare the MIPP results to previous measurements if any are available. These plots clearly illustrate that the MIPP data has unique precision, phase space coverage, and particle identification.

6. Upgrade of the experiment

Currently no decision has been made concerning a future run of the MIPP experiment. However, it is desirable to take data on nuclei that have not been measured in the first MIPP run, to extend the data to more momentum settings, to increase statistics further, and to address new physics topics. An upgrade to the MIPP experiment has been proposed in 2006 [12].

In the 2005/2006 physics run the data acquisition of the experiment was limited to $\sim 30\text{Hz}$ by the TPC read-out electronics. With modern electronics based on the

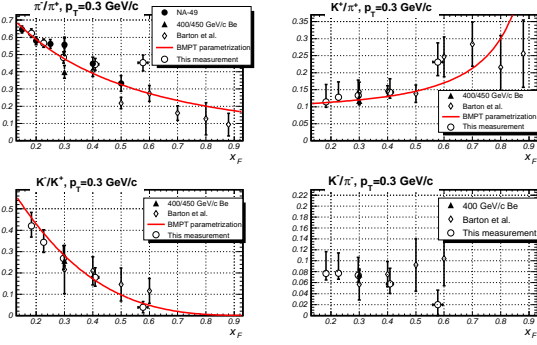


Figure 8: Ratios of π s and K s produced in reactions of $120\text{GeV}/c$ protons on a carbon target for $p_T = 0.3\text{GeV}/c$.

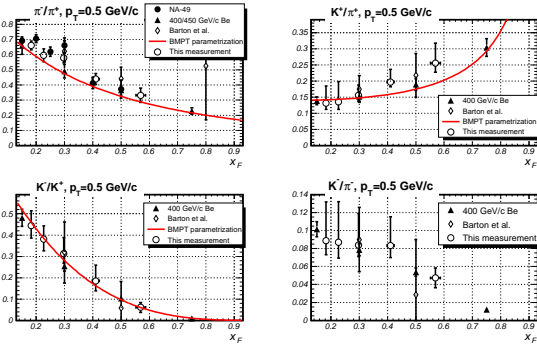


Figure 9: Ratios of π s and K s produced in reactions of $120\text{GeV}/c$ protons on a carbon target for $p_T = 0.5\text{GeV}/c$.

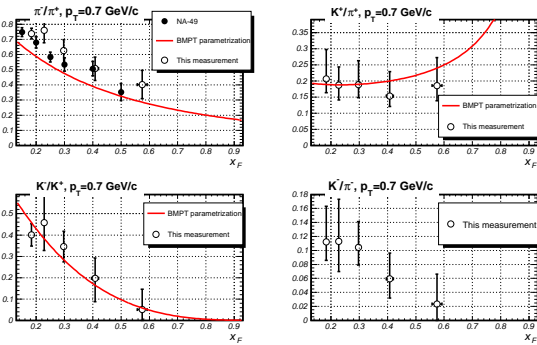


Figure 10: Ratios of π s and K s produced in reactions of $120\text{GeV}/c$ protons on a carbon target for $p_T = 0.7\text{GeV}/c$.

Altro/PASA chipset developed for the ALICE experiment at the LHC and also used by the STAR upgrade at RHIC the readout rate can be increased to $\sim 3\text{kHz}$. The Altro/PASA chips have been procured and prototype readout boards for the TPC are being tested.

With the increase by two orders of magnitude in DAQ rate the upgraded experiment will be able to acquire 5 million events per day while using less than a 5% of the Main Injector timeline.

The JGG magnet coils shorted in January of 2006 and have to be replaced. New coils have been designed to improve field uniformity in the active region of the TPC [13]. These coils have been fabricated and currently await installation in the JGG magnet yoke.

The readout electronics of the other MIPP detectors will also be replaced in the upgrade. The existing electronics for several detector subsystems are obsolete and can not be maintained for the upgrade. A common back end electronics with pipelined front-end readouts that can buffer data for a full beam slow spill will reduce the DAQ complexity and increase reliability. This approach is cost effective.

The Time of Flight and other sub-systems with TDC needs will make use of a TDC implemented in FPGA rather than ASICs [14]. Readout prototypes for both types of tracking chambers and the calorimeter are being tested. Other readout upgrades are in the design stage.

Interactions triggered with the scintillator in the first run had some contamination of uninteracted beam because the uninteracted beam leaves the signal of one minimum ionizing particle and the long Landau tail in the scintillator response is weighted up by the 1% ratio of beam to interactions resulting from a 1% interaction length target. In the upgrade we propose to trigger interactions using silicon pixels. The pixel detector will also improve vertex resolution.

Finally, we plan to add the Plastic Ball detector [15] upstream of the TPC in the backward hemisphere to detect nuclear recoil and improve acceptance of the detector. With the improved detector coverage in the backward region the MIPP experiment can be used to provide tagged neutral beams [16] to test prototype calorimeter response or measure particle production on tertiary targets. The 5 million events per day will contain tens of thousands of events (depending on momentum) of diffractive neutron, anti-neutron, or K-long production where the pion and recoil proton tag the energy of the neutral particle and the neutral particle moves in a very forward direction.

7. Conclusion

The MIPP experiment recorded a large set of data in 2005/2006. Based on this data three PhDs have been granted, first papers on detector performance have been published, and preliminary results have been shown at conferences. The complex data reconstruction is very nearly complete now and final physics publications are expected soon.

An upgrade to the MIPP experiment has been proposed and a future run of the experiment (if approved) will broaden the physics reach further.

8. Acknowledgments

The author is grateful to all colleagues on the MIPP experiment and the people at Fermilab who have made the experiment possible. I also would like to thank the organizers of BEACH2008 who hosted an interesting and pleasant conference at the University of South Carolina.

References

- [1] H. Meyer, "Physics of the MIPP Experiment", Nucl. Phys. B (Proc. Suppl.) **142** 453-8
- [2] N. Solomey, "Review of recent and future needs in hadronic flavor particle production measurements", Nucl. Phys. B (Proc. Suppl.) **167** 17-20 (2007)
- [3] M. Albrow, R. Raja (eds.), "Hadronic Shower Simulation Workshop", AIP Conference Proceedings, High Energy Physics, **896** (2007)
- [4] R. Raja, Phys. Rev. D **18** (1978) 204.
- [5] C. Amsler *et al.* (Particle Data Group), "The Review of Particle Physics", Physics Letters **B667**, 1 (2008)
- [6] H. Meyer, "The Main Injector Particle Production experiment (MIPP) at Fermilab", 2007, J. Phys.: Conf. Ser. **69** 012025 (6pp) doi: 10.1088/1742-6596/69/1/012025, MIPP-Doc-214
- [7] C. Johnstone *et al.*, "Beamline design for particle production experiment, E907, at FNAL", PAC03 conference proceedings, online at JACoW.org, <http://cern.ch/AccelConf/p03/PAPERS/TPAG011.PDF>
- [8] A. Lebedev, "Ratio of Pion Kaon Production in Proton Carbon Interactions", PhD Thesis (May 2007), MIPP-Doc-218
- [9] S. Seun, "Measurement of Pi-K Ratios from the NuMI Target", PhD Thesis (Aug. 2007), MIPP-Doc-275
- [10] N. Graf, "Measurement of the Charged Kaon Mass with the MIPP RICH", PhD Thesis (Aug. 2008), MIPP-Doc-800
- [11] T.S. Nigmanov *et al.*, "Electromagnetic and hadron calorimeters in the MIPP experiment", Nucl. Instr. and Meth. A (2008), doi: 10.1016/j.nima.2008.08.153, MIPP-Doc-729
- [12] D. Isenhower *et al.*, "Proposal to upgrade the MIPP Experiment", Fermilab Proposal P-960 (Sept. 2006), MIPP-Doc-138
- [13] H. Meyer, "JGG Field Uniformity with Extended Coils", (2006), MIPP-Doc-134
- [14] J. Wu, Z. Shi, and I.Y. Wang, "Firmware-only implementation of time-to-digital converter (TDC) in field programmable gate array (FPGA)", in *Nuclear Science Symposium Conference Record*, 2003 IEEE, **1**, 177-181
J. Wu, "MIPP TOF TDC", (2008), MIPP-Doc-847
- [15] A. Baden/emphet al., "The Plastic Ball Spectrometer – An Electronic 4Pi Detector with Particle Identification", Nucl. Instr. and Meth. **203** (1982), pp.189
- [16] R. Raja, "Tagged Neutron, Anti-Neutron and K-Long beams in an Upgraded MIPP Spectrometer", (2006), MIPP-Doc-130